Scanning probe recognition microscopy investigation of neural cell prosthetic properties

Virginia M. Ayres*, Qian Chen and Yuan Fan

Department of Electrical and Computer Engineering,
Michigan State University,
East Lansing, MI 48824, USA
E-mail: ayresv@msu.edu
E-mail: chenqia2@gmail.com
E-mail: fanywx@gmail.com
*Corresponding author

Dexter A. Flowers

Department of Electrical and Computer Engineering,
Wayne State University,
5050 Anthony Wayne Drive, Detroit, MI 48202, USA
E-mail: ay2028@wayne.edu

Sally A. Meiners and Ijaz Ahmed

University of Medicine and Dentistry of New Jersey,
675 Hoes Lane, Piscataway, NJ 08854, USA
E-mail: meiners@umdnj.edu
E-mail: iahmed999@gmail.com

Roberto Delgado-Rivera

Rutgers University,
610 Taylor Road, Piscataway, NJ 08854, USA
E-mail: robertde@eden.rutgers.edu

Abstract: Scanning probe recognition microscopy (SPRM) with auto-tracking of individual nanofibres is used for investigation of the key nanoscale properties of polyamide a nanofibrillar matrix that promotes more in vivo-like forms and functions for cultured cells. Both unmodified and fibroblast growth factor-2-modified nanofibres are considered. The contributions of nanofibrillar matrix elasticity and surface roughness to cellular behaviour are examined.

Keywords: scanning probe recognition microscopy; SPRM; adaptive scanning; basement membrane; electrospun nanofibres; fibroblast growth factor-2; FGF-2; elasticity; surface roughness.

Reference to this paper should be made as follows: Ayres, V.M., Chen, Q., Fan, W., Flowers, D.A., Meiners, S.A., Ahmed, I. and Delgado-Rivera, R. (2010) 'Scanning probe recognition microscopy investigation of neural cell prosthetic properties', *Int. J. Nanomanufacturing*, Vol. 6, Nos. 1/2/3/4, pp.279–290.

Biographical notes: Virginia M. Ayres is an Associate Professor in the Department of Electrical & Computer Engineering and heads the Electronic and Biological Nanostructures Laboratory (http://www.egr.msu.edu/ebnl) at Michigan State University. Her research interests include reduced dimensionality-based electronic properties of nanowires and nanotubes. She received her PhD and MS in Physics from Purdue University and her BAs in Physics and in Biophysics from the Johns Hopkins University.

Qian Chen received her BS and MS in Electrical Engineering from the Central South University, Changsha, China, in 1998 and 2001, respectively. She received her PhD in Electrical Engineering at Michigan State University in 2007. Her research interests include nano-bioengineering, image processing and computer vision.

Yuan Fan received his BS and MS in Electrical Engineering from Nanjing University of Aeronautics and Astronautics, Nanjing, China, in 1998 and 2001, respectively. He received his PhD in Electrical Engineering at Michigan State University in 2009. His research interests include nano-bioengineering, image processing, pattern recognition and data fusion.

Dexter A. Flowers is currently a BS candidate in Electrical and Computer Engineering at Wayne State University Detroit, Michigan, USA. He performed these studies while holding a Summer Undergraduate Research Academy Award at Michigan State University through the Michigan Louis Stokes Alliance for Minority Participation. His research interests include scanning probe microscopy and biomedical engineering.

Sally Meiners is an Assistant Professor of Pharmacology at UMDNJ-Robert Wood Johnson Medical School in Piscataway, New Jersey. She received her BS and PhD in Biochemistry at Michigan State University in East Lansing, Michigan. Her research interests include neurobiology and nanotechnology, with a special emphasis on astrocyte/neuron interactions and regulation of neuronal regeneration by naturally occurring and synthetic extracellular matrix.

Ijaz Ahmed received his Masters in Biological Sciences from the University of Saskatchewan, Canada and his PhD in Biomedical Sciences from the University of Central Lancashire, England. His research interests include neurobiology of glial cells.

Roberto Delgado-Rivera is a fourth year graduate student at Rutgers University in the Department of Chemistry and Chemical Biology. He received his BS in Industrial Biotechnology at the University of Puerto Rico, Mayagüez. His research focuses in the area of surface modification and characterisation of polymeric materials for tissue engineering applications. He has been able to perform research under a highly cross-disciplinary research program involving the areas of cellular and molecular biology, nanobiotechnoloy, polymer engineering and biointerfacial characterisation.

1 Introduction

Scanning probe microscopy (SPM) is one of the ideal techniques for nanoscale science. Its great advantages are its direct investigative capability and its inherent resolution, which easily and reliably reaches the nanometre level. But SPM has limitations in several

aspects. One limitation is slow speed of imaging, which may be due to overall system performance but may also be due to scanning outside the true region of interest. Another limitation is artefact restriction on large aspect ratio surfaces. While this limitation is typically associated with the vertical walls prevalent in semiconductor processing, another important subset is the nanoscale curved surfaces found in nanobiology.

The present investigations will use atomic force microscopy operated in a new mode, scanning probe recognition microscopy (SPRM), as a powerful new investigative tool. SPRM was developed by our group in collaborative partnership with Veeco Instruments (Woodbury, NY) (Fan et al., 2007a, 2007b; Chen et al., 2007). In SPRM, a conventional scanning probe microscope system is given the ability to auto-track on regions of interest through incorporation of recognition-based tip control. The recognition capability is realised using algorithms and techniques from computer vision, pattern recognition and signal processing fields. Adaptive learning and prediction are also implemented to make the detection and recognition procedure quicker and more reliable. The integration of recognition makes the SPRM system more powerful and flexible in investigating specific properties of samples. In the present investigations, SPRM was used to investigate mechanical and nanoscale topographical properties along individual nanofibres within tissue scaffolds composed of nanofibrillar matrices of electrospun polyamide nanofibres.

2 Results and discussion

2.1 Scanning probe recognition microscopy

An example of the difference between conventional atomic force microscopy of a nanofibrillar matrix tissue scaffold and SPRM auto-tracking along individual nanofibres within the tissue scaffold is shown in Figure 1.

Figure 1 (a) Conventional atomic force microscopy scan of a tissue scaffold (b) SPRM auto track scan along individual nanofibres in the boxed area (see online version for colours)

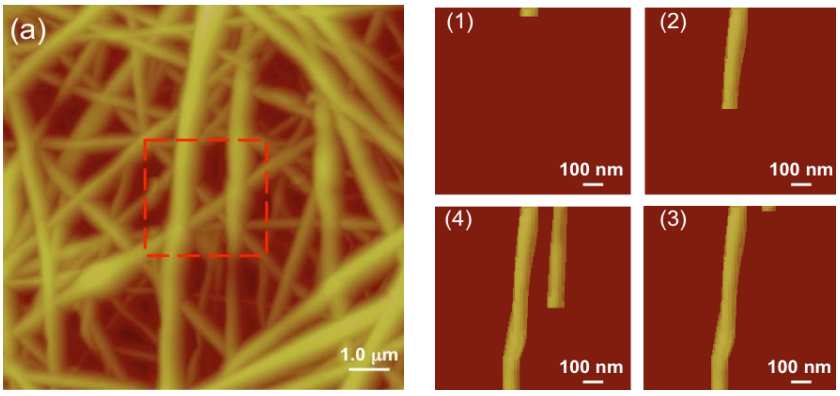

(a) (b)

In conventional atomic force microscopy, shown in Figure 1(a), a raster scan with a fixed step-size is employed throughout the image. In SPRM, shown in Figure 1(b), a user-defined coarse-step scan is initiated within user-defined boundaries [red box,

Figure 1(a)]. When a nanofibre is recognised, the instrument switches automatically into a fine-step raster scan, which proceeds trace/retrace along the full length of the nanofibre. The raster scan aspect of conventional scanning probe microscopy is maintained in SPRM to keep the benefits of piezoelectric hysteresis cancellation (http://www.physikinstrument.com/tutorial). When the end of the nanofibre (defined by the bounding box) is reached, the tip returns to the location where it left the coarse-step mode, re-enters coarse-step mode, recognises and ignores the first nanofibre and continues until it recognises a second nanofibre and begins the fine-step raster scan along its length again. An SPRM coarse and fine scan sequence for two nanofibres is shown in Figure 1(b) going clockwise (1)–(4).

Full nanofibre length scans are best for maintaining uniformity of experimental conditions during properties investigations of tissue scaffold nanofibrillar matrices. Adaptive learning that incorporated prior knowledge of likely intersection configurations and extent was used to maintain fine-step scans along individual nanofibres. An example of successful SPRM auto-tracking along an individual nanofibre past over- and under-nanofibre intersections is shown in Figure 2(a) and (b).

Figure 2 (a) Tissue scaffold nanofibrillar matrices are random nonwoven meshes with many nanofibre intersections (b) inset: SPRM auto-tracking along an individual nanofibre past over- and under-nanofibre intersections (see online version for colours)

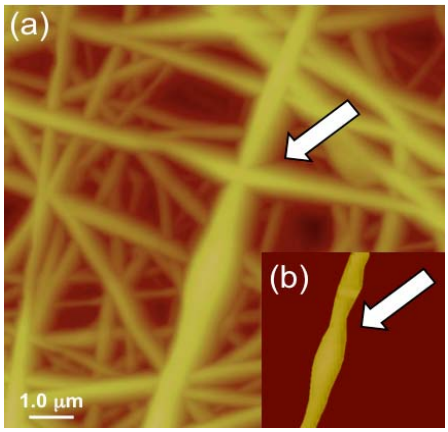

2.2 Biomedical motivation

An SPRM investigation of key nanoscale properties of a nanofibrillar matrix for neural cell culture and spinal cord repair (Ahmed et al., 2006; Meiners et al., 2007, in press) is the focus of the present research. The brain and spinal is comprised, in part, of oligodendrocytes, neurons, astrocytes and endothelial cells. Neurons are vital for such functions as cognition, memory and emotion, which are largely facilitated through neurotransmission between axons on pre-synaptic cells and dendrites or somas on post-synaptic cells. Finally, endothelial cells with special adaptations form central nervous system capillaries. A sheet of basement membrane surrounds each capillary and aids in reducing its permeability.

Investigations by Meiners' group indicate that a synthetic polyamide nanofibrillar matrix prepared via electrospinning (Rutledge et al., 2006; Dzenis, 2004) can promote

more *in vivo*-like functions for astrocytes; specifically, astrocytes cultured on nanofibres become more permissive substrates for neurite outgrowth when cultured with an overlay of neurons (Delgado-Rivera et al., 2009). This property increases with the addition of FGF-2. This is highly relevant in that the FGF-2-modified nanofibrillar matrix geometrically and chemically mimics the basement membrane that separates astrocytes from endothelial cells at the blood brain barrier. Importantly, research by Meiners' group has demonstrated that FGF-2 retains biological activity significantly longer when immobilised on nanofibres than when presented to cells as a soluble molecule (Nur-E-Kamal et al., 2008). Details of the covalent modification, cross-linking a neuroactive group to an amine base on nanofibres coated with a proprietary polyamine coating (Surmodics, Inc., Eden Prairie, MN)), are given in (Ahmed et al., 2006). A tapping mode atomic force microscopy image of typical FGF-2-modified nanofibres is shown in Figure 3; it indicates dense FGF-2 coverage.

Figure 3 Tapping mode atomic force microscopy image of covalent modification of nanofibres with FGF-2 (see online version colours)

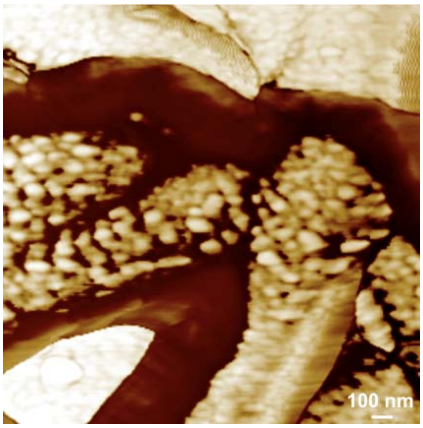

2.3 Properties investigation by SPRM

The aim of the present SPRM research is to quantify the material properties and organisation of the nanofibres to understand how it successfully mimics the basement membrane at the blood-brain barrier. The key properties that can be investigated using SPRM include nanofibre elasticity, surface roughness, curvature, mesh density and porosity, and growth factor distribution. Each of these factors has been demonstrated to have global effects on cell morphology, function, proliferation, morphogenesis, migration and differentiation. The present work will focus on elasticity and surface roughness and how these properties are changed by FGF-2 modification.

Several research groups have recently produced evidence that local elasticity strongly influences cell attachment and growth (Georges et al., 2006; Discher et al., 2005; Engler et al., 2006; Guo et al., 2006), including neural cell attachment and oriented growth (Georges et al., 2006). SPRM was used to directly evaluate elasticity along individual nanofibres within the nanofibrillar matrix for unmodified and FGF-2-modified samples. SPRM-based local force volume imaging along the nanofibre medial axis was performed using silicon nitride tips with a nominal tip radius of 20 nm and a nominal spring constant

0.58 N/m. The trace portion of an SPRM fine-scan was used to identify the nanofibre boundaries. Nano-indentation (local force volume imaging) was performed during retrace at the nanofibre midpoint. The indentation was set to 300 nm lift and 302 nm descent. These experiments were performed in ambient air at room temperature (typically used to assess polymer sample elastic moduli).

A Hertz model was used to quantify the contact (extension) part of the force curve generated. The Hertz model describes the elastic deformation of two surfaces touching under a load force. The general force-indentation relation can be expressed as

$$F = \lambda\delta^{\beta} \tag{1}$$

where F is the loading force and δ is the indentation depth. The term λ and exponent β are parameters decided by the two touching surfaces. For normal nano-indentation achieved through SPRM, an individual nanofibre surface can be considered as a flat soft sample. Since the tip is much harder than the sample, the elastic deformation of the sample can be related to its Young's modulus in the contact part of the force curve. When the tip geometry is described as a sphere of radius R (estimated by tip characterisation), the Hertz model is defined as:

$$F_{sphere} = \frac{4}{3}\frac{E}{(1-\mu^2)}\sqrt{R}\delta^{3/2} \tag{2}$$

where F_{sphere} is the measured force, E is the Young's modulus, μ is the Poisson's ratio and δ is the indention depth. The indentation δ is calculated as follows:

$$\delta = (z - z_0) - (d - d_0) \tag{3}$$

where z is the sample height, z_0 is the contact point where tip touches the sample, d is the cantilever deflection and d_0 is the deflection of the free cantilever when the cantilever is far from the sample surface. To simply the problem, the nonlinear force (F_{sphere}) and indentation (δ) equation is converted to linear equation for $(F_{sphere})^{2/3}$ and δ by substituting equation (3) into equation (2):

$$F_{sphere}{}^{2/3} = (\frac{4}{3}\frac{E}{(1-\mu^2)}\sqrt{R}^{2/3}[(z - z_0) - (d - d_0)] \tag{4}$$

In equation (4), F_{sphere}, z, d and d_0 can be obtained from the experimental force curves. Typically, the Poisson's ratio μ can be assumed as 0.5 for soft materials. The unknown parameters are Young's modulus E and the tip-sample contact point position z_0. In this work, we use a least squares estimation procedure to determine E and z_0 by minimising the RMS error σ in equation (4) with respect to unknown parameters E and z_0:

$$\sigma = \sqrt{\frac{1}{N}\sum_{i=1}^{N}((F_{sphere}^{th})^{2/3} - (F_{sphere}^{\exp})^{2/3})^2} \tag{5}$$

Sigma σ is the RMS error, $F_{sphere}^{\exp}$ is the measured force in contact region and F_{sphere}^{th} is the force calculated using equation (4). It is noted that a curved cylindrical nanofibre surface has a highly restricted region of interest (ROI) for elasticity property measurements using the Hertz model, which is the single median point where the tip is

exactly normal to the nanofibre surface. This condition was met by using SPRM.

Results are shown in Figure 4 as a box plot, in which the red line is the mean elasticity and the blue box is the variance. The measured elastic moduli values are comparable to those found in brain tissue (Miller et al., 2000); however, it is noted that the absolute numbers are cautionary as appropriate calibration for the polyamide nanofibre material versus the hollow core nanofibre tension are under investigation by our group.

Figure 4 SPRM nano-indentation normal to the nanofibre axis was performed over multiple unmodified and FGF-2 modified nanofibres, as shown on the left; box plot of mean values with variances, shown on the right, indicates that the Young's modulus is reduced by FGF-2 modification (see online version for colours)

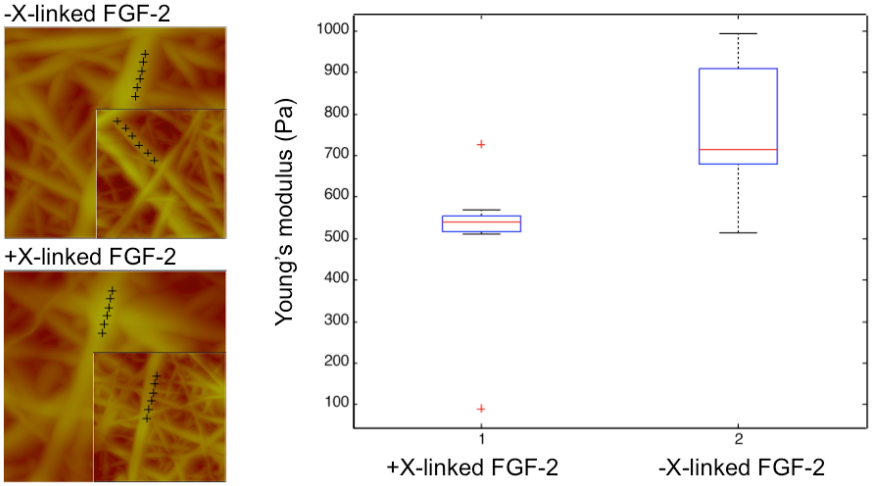

Comparisons of the measured values show the following trends. The mean elasticity of the FGF-2 modified nanofibres was reduced by ~25% relative to the unmodified nanofibres. The variance was substantially reduced by the FGF-2 modification, by a factor of ~10.

These trends indicate that covalent modification of the nanofibre surfaces by FGF-2 may significantly alter the elasticity perceived by an approaching neural cell extension and that the sense of the change is toward a reduction in the elasticity and also a reduction in its variance (or an increase in its uniformity).

The quantitative elastic moduli estimates can be examined in the context of neural cell responses, using data from our groups and others. A picture is emerging (Discher et al., 2005; Vogel and Sheetz, 2006) that cells actively probe the mechanical aspect of their environments by exerting self-generated local forces on it [traction stresses, force/area (Discher et al., 2005)]. Neuron studies indicate that these cells preferentially select softer substrates but can attach and develop functional axons on both hard and soft substrates (Georges et al., 2006). This has been attributed to relatively weak local traction forces generated by neural growth cones.

Astrocytes have been noted for a strong response to the mechanical environment, which is attributed to strong local probing forces generated by these actin-based cells. Astrocyte studies indicate that these cells preferentially select harder substrates (to the

extent of becoming invasive) and are inhibited by softer ones (Georges et al., 2006). However, our results indicate that the FGF-2 modification promotes more biologically relevant phenotypes for cultured astrocytes than unmodified nanofibres in vitro (Delgado-Rivera et al., 2009). Further SPRM studies of elastic moduli variations in physiological ambient and temperature, and neuron and astrocyte cell responses are continuing within our group.

The effects of surface roughness on cells have been investigated mainly for osteoblasts on hydroxy apatite (Deligianni et al., 2001) and titanium (Zhao et al., 2007), both used as replacements for bone. A positive correlation was demonstrated for hydroxy apatite and mixed results for titanium. However, investigations of embryonic vascular and corneal cells on poly (methyl methacrylate) substrates indicated that surface roughness may have a strong effect by indirect means: through alteration of surface hydrophobicity/philicity (lotus leaf effect) and through promotion of protein adhesion by surface roughness variation (Lampin et al., 1997).

The role of the nanoscale surface roughness of nanofibrillar matrices for neural cell attachment and motility is under consideration for the first time by our group. Two important points for working with the surface roughness property of nanofibres in meshes were noted during these investigations. The first point is that the variation of the raw height data, Z, includes not only the surface roughness variation, but also the variation caused by the cylindrical curvature. Therefore, distance data, D, instead of height data, Z, was used to determine the real roughness of the nanofibre surfaces. The Kåsa circle fit method (Kåsa, 1976) was implemented to get the centre of the most fitted circle as shown in Figure 5.

Figure 5 Deconvolution by the mathematical morphology method with a Kåsa circle fit was used to estimate the nanofibre curvature for accurate surface roughness measurements (see online version for colours)

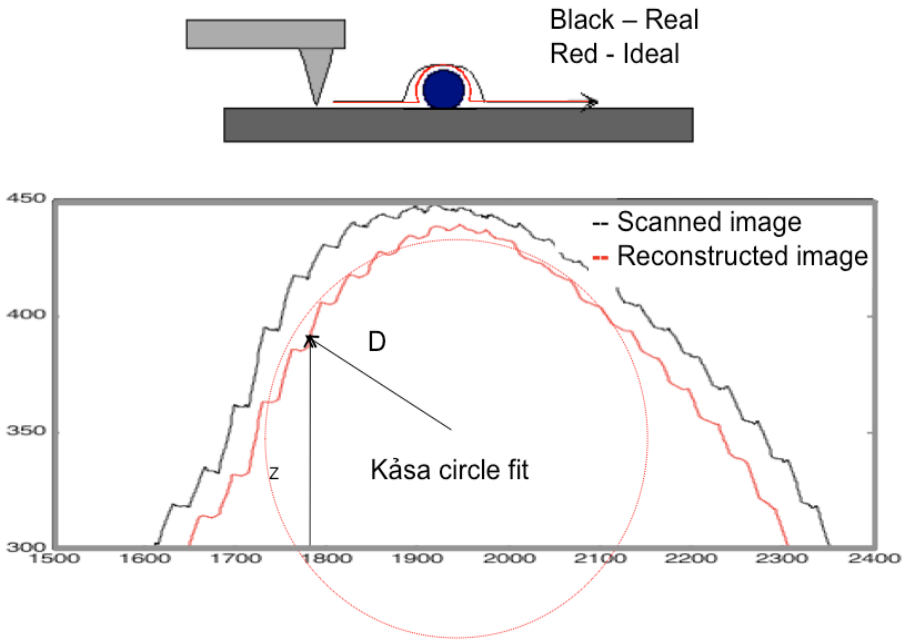

Therefore, the distance

$$D_i = \sqrt{(Z_i - Z_{center})^2 + (X_i - X_{center})^2} \tag{6}$$

between each point on the surface and the centre was evaluated and used to calculate the surface roughness maps and statistical surface roughness histograms (Fan et al., 2007a). The second point is that a cylindrical nanofibre surface also has a ROI for surface roughness measurements based on height (distance) values. The correct ROI for surface roughness measurements is the arc where the apex of the tip is in interaction with the sample surface. Side-of-the-tip interaction corresponds to the well-known dilation artefact. An erosion operation may be applied as the inverse operation to reverse the tip-shape dilation artefact. In work described in Udpa et al. (2006), we have investigated the uses of mathematical morphology methods for automated erosion based on deconvolution by mathematical morphology methods (Villarrubia, 1997). Basic concepts of set theory such as union, subset, intersection, translation and mutual exclusivity are used for the defining operations in the mathematical morphology method. An intersection of the deconvolution trace with the raw SPRM trace was used to identify a high-confidence arc free of the dilation artefact. A Kåsa circle fit can then be used as an estimate for true nanofibre diameter and curvature measurements and statistics. Because individual nanofibres are on top of other nanofibres in a tissue scaffold mesh, it is impossible to use the usual height measurement on a flat substrate to accurately assess their height (diameter). Thus, SPRM can be used to enable a property measurement in a previously inaccessible situation.

Using data obtained by SPRM along individual nanofibres within the true-curvature ROI, the RMS surface roughness was calculated according to

$$RMS = \sqrt{\frac{\sum_{i=1}^{N} (D_i - D_{ave})^2}{N}} \tag{7}$$

$$D_{ave} = \frac{1}{N} \sum_{i=1}^{N} D_i \tag{8}$$

on each pixel based on a user-defined local neighbourhood box. In these experiments a rectangular box close to the nanofibre ROI was selected. Multiple sets of overlapping calculations were thus generated with the provision that any box that extended beyond the ROI was automatically truncated.

Results from the SPRM investigation of the surface roughness property over multiple nanofibres in are shown in Figure 6. Histograms instead of box plots were analysed to investigate whether the FGF-2 modification would affect shape of the surface roughness distribution curve (Fan et al., 2007a). The shape of the distribution curve for the unmodified nanofibrillar matrix, top right, was bimodal. While the mode RMS surface roughness value (the value returned most often) was low, ~3 nm, a second strong population of ~7 nm values was observed, and the distribution curve included a long tail of even higher RMS surface roughness values up to ~15 nm. This distribution curve is similar to one previously analyzed in Fan et al. (2007a), for 'typical' hollow core electrospun nanofibres. Two effects from FGF-2 modification were observed

(comparison of the upper right and lower right figures). One was an increase in the RMS surface roughness mode value from ~3 to ~5 nm. The other was a change in the shape of the distribution curve towards a more compact single mode distribution. Thus, overall, the effect of the FGF-2 modification has been to increase the RMS surface roughness but also to increase its uniformity.

Figure 6 Survey AFM of analysis regions, unmodified (top row) and FGF-2 modified (bottom row) shown on the left; SPRM surface roughness maps along individual nanofibres shown middle; histograms and distributions (dotted lines) based on multiple unmodified and FGF-2 modified nanofibres (see online version for colours)

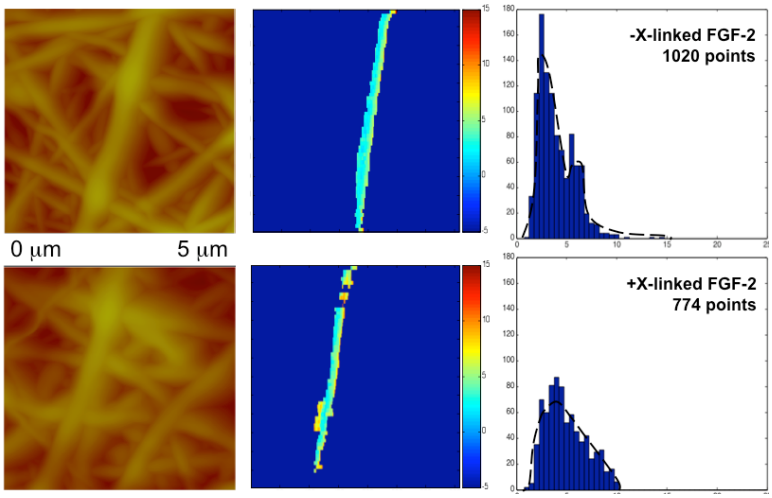

2.4 Implications for nanomanufacturing

Elasticity and surface roughness investigations were performed using atomic force microscopy operated in the new SPRM mode. SPRM auto-tracking along multiple individual nanofibres enabled measurements of mechanical and nanoscale topographical properties that were improved in three ways:

1 The most reliable data points were accessed and utilised.

2 Statistically meaningful numbers of reliable data points were extracted providing ranges and distributions for each property.

3 All data was extracted using an automatic procedure that maintains uniformity of experimental conditions.

As noted above, the elasticity and surface roughness properties are part of a set of key properties under SPRM investigation, which include nanofibre stiffness and surface roughness, nanofibre curvature, nanofibre mesh density and porosity and growth factor presentation and distribution. They are likely to act synergistically, i.e., surface chemistry affecting elasticity and surface roughness affecting surface chemical modification. Results from this research are likely to have an immediate impact on tissue engineering development aimed at recreating the neural cell system following central nervous system injury. For example, results from these studies may enable the nanoscale design of an

optimised scaffolding material that will encourage astrocyte re-population of an injury site in the damaged central nervous system, which will in turn promote axonal regeneration. Further, as scaffold-based cell systems are ubiquitous throughout the body, these investigations can serve as the basis for quantitative exploration of other regenerative cell-scaffold systems. First SPRM investigations in which the important elasticity property was correlated with electrospinning conditions for a series of electrospun nanofibres demonstrate the feasibility and the potential of this approach. As shown in Figure 7, we envision the use of SPRM as an integral part of an accurate and efficient manufacture of tissue scaffolds with nanoscale properties that are appropriate for diverse cells types.

Figure 7 SPRM as an integral part of accurate and efficient nanomanufacture of tissue scaffolds with appropriate nanoscale properties for diverse cells types (see online version for colours)

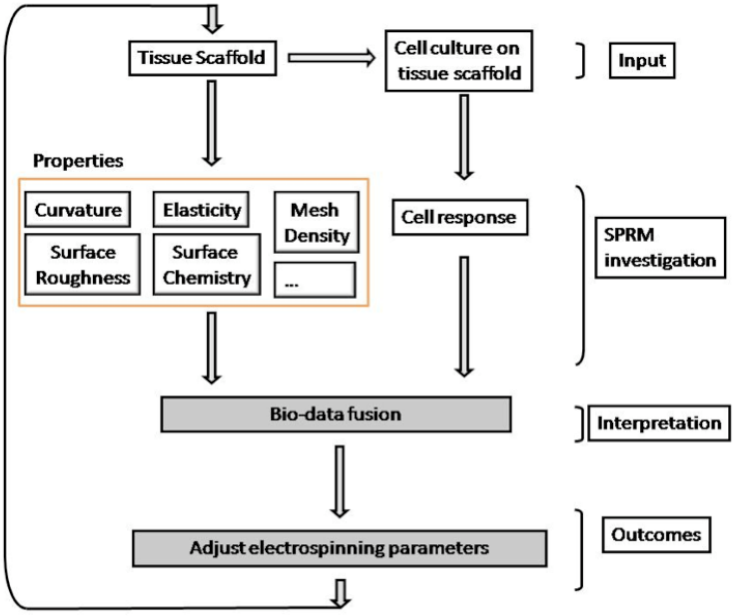

Acknowledgements

This work was supported by National Science Foundation Grant DMI-0400298 to V.M. Ayres and by the New Jersey Commission on Spinal Cord Research Grant 06A-007-SCR1 and funds from Donaldson Co., Inc., to S.A. Meiners. R. Rivera-Delgado gratefully acknowledges the Rutgers-National Science Foundation Integrative Graduate Education and Research Traineeship (IGERT) Program on Integratively Engineered Biointerfaces. D. Flowers gratefully acknowledge the Michigan-Louis Stokes Alliance for Minority Participation program. The polyamide nanofibres (Ultra-WebTM) described in this work was produced by Donaldson Co., Inc. (Minneapolis, MN, USA).

References

Ahmed, I., Liu, H-Y., Mamiya, P.C., Ponery, A.S., Babu, A.N., Weik, T. and Meiners, S.J. (2006) *Biomed. Mater. Res. A*, Vol. 76, pp.851–856.

Chen, Q., Fan, Y., Kumar, S., Baczewski, A.D., Udpa, L., Ayres, V.M., Rice, A.F., Meiners, S. and Ahmed, I. (2007) *Mater. Res. Soc. Symp. Proc.*, Vol. 1019E, 1019-FF06-04.

Delgado-Rivera, R., Harris, S.L., Ahmed, I., Babu, A.N., Patel, R., Ayres, V.M., Flowers, D.A. and Meiners, S. (2009) *Matrix Biology*, in press, online epub ahead of print available 23 February 2009.

Deligianni, D.D., Katsala, N.D., Koutsoukos, P.G. and Missirlis, Y.F. (2001) *Biomaterials*, Vol. 22, pp.87–96.

Discher, D.E., Janmey, P. and Wang, Y-L. (2005) *Science*, Vol. 310, pp.1139–1143.

Dzenis, Y. (2004) *Science*, Vol. 304, pp.1917–1919.

Engler, A.J., Sen, S., Sweeney, H.L. and Discher, D.E. (2006) *Cell*, Vol. 126, pp.677–689.

Fan, Y., Chen, Q., Ayres, V.M., Baczewski, A.D., Udpa, L. and Kumar, S. (2007a) *Int. J. Nanomedicine*, Vol. 2, pp.651–661.

Fan, Y., Chen, Q., Kumar, S., Baczewski, A.D., Udpa, L., Ayres, V.M. and Rice, A.F. (2007b) *Mater. Res. Soc. Symp. Proc.*, Vol. 1021E, 1021-HH05-26.

Georges, P.C., Miller, W.J., Meaney, D.F., Sawyer, E.S. and Janmey, P. (2006) *Biophys. J.*, Vol. 90, pp.3012–3018.

Guo, W-H., Frey, M.T., Burnham, N.A. and Wang, Y-L. (2006) *Biophys. J.*, Vol. 90, pp.2213–2220.

http://www.physikinstrument.com/tutorial, 'Theory an applications of piezo actuators and PZT nanopositioning systems'.

Kåsa, I. (1976) *IEEE Trans. Inst. Meas.*, Vol. 25, pp.8–14.

Lampin, M., Warocquier-Cle, R., Legris, C., Degrange, M. and Sigot-Luizard, M.F. (1997) *J. Biomed. Mater. Res.*, Vol. 36, pp.99–108.

Meiners, S., Ahmed, I., Ponery, A.S., Amor, N., Ayres, V.M., Fan, Y., Chen, Q. and Babu, A.N. (2007) *Polymer Int.*, Vol. 56, pp.1340–1348.

Meiners, S., Harris, S.L., Delgado-Rivera, R., Ahmed, I., Babu, A.N., Patel, R.P. and Crockett, D.P. (in press) 'A nanofibrillar prosthetic modified with fibroblast growth factor-2 for spinal cord repair', in *Nanofibers: Fabrication, Performance and Applications*, W.N. Chang (Ed.), Nova Science Publishers, Inc., Hauppage, NY.

Miller, K., Chinzei, K., Orssengo, G. and Bednarz, P.J. (2000) *Biomech*, Vol. 33, pp.1369–1376.

Nur-E-Kamal, A., Ahmed, I., Babu, A.N., Kamal, J., Schindler, M. and Meiners, S. (2008) *Mol Cell Biochem.*, Vol. 309, pp.157–166.

Rutledge, S.L., Shaw, H.C., Yowell, L.L., Chen, Q., Jacobs, B.W., Song, S.P. and Ayres, V.M. (2006) *Diamond and Relat. Mater.*, Vol. 15, pp.1070–1074.

Udpa, L., Ayres, V.M., Fan, Y., Chen, Q. and Arun-Kumar, S. (2006) *IEEE Sig. Proc. Mag. Special Issue on Molecular and Cellular Bioimaging*, Vol. 23, pp.73–83.

Villarrubia, J.S. (1997) *J. Res. Natl. Inst. Standards Technol.*, Vol. 102, pp.425–454.

Vogel, V. and Sheetz, M. (2006) *Nature Reviews: Molecular Cell Biology*, Vol. 7, pp.265–275.

Zhao, B.H., Lee, I-S., Han, I.H., Park, J-C. and Chung, S-M. (2007) *Curr. Appl. Phys.*, Vol. 7S1, pp.e6–e10.